
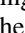


Optimal quantum resource generation by coupled transmons immersed in Markovian bathsTanaya Ray , Ahana Ghoshal, Debraj Rakshit, and Ujjwal Sen *Harish-Chandra Research Institute, A CI of Homi Bhabha National Institute, Chhatnag Road, Jhansi, Prayagraj 211 019, India*

(Received 13 June 2023; accepted 23 October 2023; published 16 November 2023)

We analyze quantum resource generation of capacitively coupled multilevel transmon circuits surrounded by bosonic baths, within the Markovian limit. Superconducting circuit elements are in practice usually part of a larger circuit, constructed with many other elements, which along with their environment is assumed to be mimicked by the baths. We study the response, to variation of the temperature of the thermal baths and the coupling strength, of resource generation for the system prepared in zero-resource initial states. We focus, in particular, on entanglement and quantum coherence as resources. We find that capacitive coupling, even if weak, can compete with Markovian decay of quantum resources and lead to significant steady-state values of the same. At short and moderate timescales, the resources exhibit nonmonotonic oscillatory behavior, reminiscent of the same in non-Markovian environs in absence of intrasystem coupling. We quantify the entanglement generation power of coupled transmon qutrits, taking into account the maximum entanglement the system can generate and the timescale over which the system can sustain a significant amount of the same. We identify the optimal initial separable states leading to maximum entanglement generating power.

DOI: [10.1103/PhysRevA.108.052417](https://doi.org/10.1103/PhysRevA.108.052417)**I. INTRODUCTION**

In recent years, quantum information processing has become an important field of research due to its wide-ranging applications in quantum techniques such as computational speedup [1–3] and cryptographic security [4]. Quantum computers can potentially be realized with trapped ions [5,6], superconducting qubits [7–14], photons [15–19], silicon chips [20,21], etc. The superconducting Josephson-junction qubit [22–25] is a leading candidate for the experimental realization of quantum computers. These superconducting systems derived from Josephson junctions, separated, or joined by carefully chosen circuit elements, can primarily be divided into three subclasses according to their degree of freedom exploited to realize the qubit, viz., charge [26,27], flux [28,29], and phase [30]. But short coherence times pose a major challenge in extracting the optimal performances from such systems.

The transmon, a superconducting qubit, has been proposed as a promising physical substrate for overcoming this limitation [31]. The structure of a transmon qubit is very similar to the Cooper pair box (CPB) qubit [26] shunted with a large capacitor, and its ratio of Josephson energy to charging energy, E_J/E_C , lies in between that of charge and phase qubits. Two important parameters of a transmon qubit, viz., anharmonicity and charge dispersion of the energy levels, are usually determined by this ratio [32–35]. The anharmonicity should be sufficiently large in order to prevent qubit operations from exciting other transitions in the system. Consequently, the charge dispersion needs to be reduced to minimize the system's sensitivity to charge noise due to change in gate charge and stray electric fields [36]. In a transmon qubit, the charge dispersion of the energy levels decreases exponentially with E_J/E_C and the anharmonicity of the same reduces algebraically with a slow power law of E_J/E_C [37]. Hence, in order to obtain the suitable operating regime of a transmon

qubit, the ratio E_J/E_C has to be chosen properly. For experimental realization of transmon qubits, see [38–51].

Entanglement [52–54] and quantum coherence [55–58] are two important resources for quantum information processing. The presence of environment influences the effective operating time of a transmon, resulting in a shorter coherence time. The coherence times of transmon qubits have been rigorously studied in previous literature in presence of various Markovian [59] and non-Markovian [60,61] environments. Entanglement between coupled transmon qubits has also been studied [62–71].

In this paper, we consider two capacitively coupled transmon qutrits, locally surrounded by harmonic oscillator baths. This setup provides not only a realistic setup, but also, interestingly, can self-generate quantum resources in the system, evolving from zero-resource initial states. We observe that an increased temperature gap between the two local baths accelerates the decay of quantum resources of the two-transmon system. We also show enhancement in the generation of the quantum resources with increasing coupling strength. The maximum attainable as well as the long-time values of the quantum resources generated by the system increase almost linearly with the increase in the strength of capacitive coupling, restricting ourselves to the regime of weak to moderate coupling strength between the subsystems. We study the entanglement generating power of such a coupled transmon setup, which depends on the maximum entanglement the system can generate, and the timescale over which the system can sustain this self-generated entanglement to a significant amount. Furthermore, we find the optimal initial separable states of the composite system providing the maximum entanglement generating power, for small strengths of capacitive coupling between the two transmon qutrits.

The rest of the paper is arranged as follows. In Sec. II, we describe the system under study. In Sec. III, we discuss

measures of the quantum resources that we analyze in this paper. Section IV presents the results of quantum resource generation in the coupled-transmon system, for certain classes of paradigmatic initial states. In Sec. V, we define the maximum entanglement generating power of the system, and compute the optimal initial separable states that can generate maximum entanglement in presence of Markovian baths for fixed sets of system and bath parameters. A conclusion is presented in Sec. VI.

II. TRANSMONS COUPLED THROUGH CHARGE-CHARGE INTERACTION

Structurally, a transmon is close to a Cooper pair box [23], and it can be constructed by two superconducting islands (or one island and ground), coupled through a Josephson junction and isolated from all other elements of the circuit [31]. The system is described by a pair of canonically conjugate quantum operators constructed from the number of Cooper pairs transferred through the junction and the phase across it. The charge-based systems are sensitive to stray electric-field noise. This unwanted situation can be largely overcome by putting the Cooper pair box in the “transmon” regime, where the Josephson tunneling energy dominates over the Coulomb charging energy [10,30,31,72–75].

The effective Hamiltonian of a CPB in the transmon regime can be written as [31,76]

$$H_{\text{tr}} = 4E_C \hat{n}^2 - E_J \cos \hat{\phi}, \quad (1)$$

where $E_J = I_0 \Phi_0 / 2\pi$ is the Josephson energy and $E_C = \frac{e^2}{2C}$ is the charging energy. Here we ignore the offset (or “gate”) charge, given that the system is not sensitive to the offset charge in the transmon regime. $\hat{n} = \hat{Q}/2e$ is the reduced charge operator ($2e$ being the charge content of a Cooper pair) and $\hat{\phi} = 2\pi \Phi / \Phi_0$ is the phase ($\Phi_0 = h/2e$ being the flux quanta) operator for the number of Cooper pairs and the phase across the Josephson junction, respectively. Here, h is Planck’s constant. I_0 is the maximum current allowed through the Josephson junction maintaining the superconducting state and C is the total capacitance of the transmon circuit to its environment. The current (I) and flux (Φ) across the Josephson junction are connected by the following Josephson relation:

$$I = I_0 \sin(2\pi \Phi / \Phi_0). \quad (2)$$

Quantization of this system is approached by constructing the ladder operators in terms of the zero-point fluctuations of charge and phase as

$$\hat{n} = in_{\text{ZPF}}(\hat{c}^\dagger - \hat{c}) \quad \text{and} \quad \hat{\phi} = \phi_{\text{ZPF}}(\hat{c}^\dagger + \hat{c}),$$

with $n_{\text{ZPF}} = (E_J/32E_C)^{\frac{1}{4}}$ and $\phi_{\text{ZPF}} = (2E_C/E_J)^{\frac{1}{4}}$. The operator $\hat{c} = \sum_j \sqrt{j+1} |j\rangle \langle j+1|$ is the transmon annihilation operator and the \hat{c}^\dagger is the corresponding transmon creation operator. Note that the action of \hat{n} provides integer values and changes by ± 1 when a Cooper pair tunnels through the Josephson junction. In the transmon regime, $E_J/E_C \gg 1$, and hence $\hat{\phi} \ll 1$, providing the opportunity to simplify the Hamiltonian by expanding $\cos \hat{\phi}$ in Taylor series and then approximating the expression by ignoring small higher-order contributions. If we retain terms up to second order in $\hat{\phi}$

only, and then express the canonical operators in terms of the raising or lowering operators, the transmon Hamiltonian is approximated as

$$H_T \approx \sqrt{8E_C E_J} \left(\hat{c}^\dagger \hat{c} + \frac{1}{2} \right) - \frac{E_C}{12} (\hat{c}^\dagger + \hat{c})^4 - E_J. \quad (3)$$

This Hamiltonian resembles that of a quantum oscillator in a harmonic potential modified by a comparatively smaller quartic potential. One can solve this by using certain variational techniques, such as the “explicitly correlated Gaussian method” [77]. Consistent results have been obtained if this quartic term is treated perturbatively in the transmon regime ($E_J \gg E_C$), or solved using the explicitly correlated Gaussian method.

In this paper, we consider a pair of coupled transmon qutrits. Thus, we concentrate on three lowest-energy states of a multilevel transmon. We study the global quantum coherence of the combined system and the bipartite entanglement between the qutrits. The two transmons are coupled via an electric field. This type of coupling occurs when the individual transmon circuits are coupled through an electric field via a capacitor. This is particularly plausible when the impedance of the source circuit is high [31,78,79]. This kind of interaction between two transmons can be modeled as [12,80]

$$H_{\text{int}} = \hbar \gamma \hat{n}_1 \hat{n}_2 = -\hbar \frac{\gamma}{\sqrt{32}} \left(\frac{E_{J_1} E_{J_2}}{E_{C_1} E_{C_2}} \right)^{\frac{1}{4}} (\hat{c}_1^\dagger - \hat{c}_1)(\hat{c}_2^\dagger - \hat{c}_2). \quad (4)$$

Here we neglect the charge offset terms, since the transmon regime provides us with the charge-insensitive (insensitive to gate charge) regime to work in. The coupling constant γ is taken to be roughly one order of magnitude smaller than the first excitation energy of a single transmon qutrit (the energy required for a transition from the ground state to the first excited state), in view of the fact that this kind of coupling is often weak compared to the energy scales of the individual systems. The Hamiltonian of this composite two-transmon system is taken as

$$H_s = \sum_{i=1}^2 \left[\hbar \omega_{0_i} \left(\hat{c}_i^\dagger \hat{c}_i + \frac{1}{2} \right) - \frac{E_{C_i}}{12} (\hat{c}_i^\dagger + \hat{c}_i)^4 \right] + H_{\text{int}}, \quad (5)$$

where $\omega_{0_i} = \sqrt{8E_{C_i} E_{J_i}} / \hbar$ ($i = 1, 2$). Here, we have dropped the constant contributions coming from E_{J_1} and E_{J_2} [see Eq. (3)] as these terms just give a constant shift to all energy values. In all the further discussions of this paper, we have taken $E_{J_1} = E_{J_2} \equiv E_J$, $E_{C_1} = E_{C_2} \equiv E_C$, and $\omega_{0_1} = \omega_{0_2} \equiv \omega_0 = \sqrt{8E_C E_J}$.

III. MEASURES OF QUANTUM RESOURCES

Our aim in this paper is to investigate the dynamics of various quantum resources, in particular of quantum coherence and quantum entanglement, in the system studied. Of these two resources, quantum coherence is a basis-dependent quantity, while entanglement is basis independent. In this paper, the l_1 -norm of quantum coherence and logarithmic negativity are chosen as the quantum coherence and entanglement measures, respectively.

A. l_1 -norm of quantum coherence

The l_1 -norm of quantum coherence of an arbitrary d -dimensional state ρ , possibly mixed, is defined as the sum of the moduli of the off-diagonal terms, when the state is expressed in a fixed reference basis [55–58]. Let us consider a d -dimensional Hilbert space \mathbb{C}^d and fix a basis of it, $\{|i\rangle\}$, for $i = 1, 2, \dots, d$, as the reference basis. Then, the l_1 -norm of quantum coherence of an arbitrary d -dimensional quantum state $\rho = \sum_{i,j} p_{ij} |i\rangle\langle j|$, with respect to the basis $\{|i\rangle\}$, is given by $\tilde{C}_{l_1}(\rho) = \sum_{i \neq j} |p_{ij}|$.

The maximum value of the l_1 -norm of quantum coherence of a state on \mathbb{C}^d is given by $\tilde{C}_{l_1 \max} = (d^2 - d)/d = d - 1$. So, in order to normalize the obtained value of quantum coherence, and make the maximum dimension independent, $\tilde{C}_{l_1}(\rho)$ is rescaled by $\tilde{C}_{l_1 \max}$. In this paper, we consider the states on the Hilbert space constructed from the three lowest-lying states of each of the two coupled transmon systems. The two-transmon states are therefore defined on $\mathbb{C}^3 \otimes \mathbb{C}^3$, and so, $\tilde{C}_{l_1 \max} = 8$. Hence, the expression of the l_1 -norm of quantum coherence, taken in all further considerations of this paper, is given by

$$C_{l_1}(\rho) = \frac{1}{8} \sum_{i \neq j} |p_{ij}|. \quad (6)$$

The maximum value of $C_{l_1}(\rho)$, therefore, reaches to unity in the $\mathbb{C}^3 \otimes \mathbb{C}^3$ system. This l_1 -norm of quantum coherence, normalized by the quantum coherence of a maximally coherent density matrix in the same Hilbert space, expresses the quantum coherence of the system in the unit of cobits [81–83].

B. Logarithmic negativity

One of the most popular measures of bipartite entanglement is the logarithmic negativity [84,85]. Suppose, ρ is a two-party (A and B) density matrix and ρ^{T_A} is the partial transpose of ρ on the subsystem A . The negativity of the density matrix ρ is defined as

$$\mathcal{N}(\rho) = \frac{\|\rho^{T_A}\|_1 - 1}{2}. \quad (7)$$

Here, the trace norm of an operator A stands for $\|A\|_1 = \text{Tr}(\sqrt{A^\dagger A})$. This $\mathcal{N}(\rho)$ presents the absolute value of the sum of negative eigenvalues of ρ^{T_A} [86,87]. The logarithmic negativity of ρ is now defined as

$$\mathcal{L}_{\mathcal{N}}(\rho) = \log_2[2\mathcal{N}(\rho) + 1]. \quad (8)$$

If ρ is a maximally entangled state, then $\mathcal{L}_{\mathcal{N}}(\rho)$ equals 1 ebit. Here, an ‘‘ebit,’’ short for ‘‘entanglement bit,’’ is a unit of entanglement for bipartite quantum systems.

IV. RESOURCE GENERATION IN A PAIR OF COUPLED TRANSMON QUTRITS

In this section we investigate the variation of quantum coherence and entanglement for different initial states of a pair of interacting transmon qutrits described by the Hamiltonian H_s [see Eq. (5)]. We consider two different situations. First, for completeness, we consider the unitary evolution of the isolated system solely governed by the Hamiltonian H_s . Next, we investigate the scenario where each transmon qutrit

is locally connected to a bosonic bath within the Markovian limit. We consider weakly coupled harmonic baths, where the coupling between a transmon and a bath is weak and the baths are infinitely large, having a continuously distributed energy spectrum, for the validation of the Born-Markov approximations [88–91].

A. Coupled transmons isolated from the environment

We now present the time dynamics of quantum resources in the system described, isolated from any environmental effects. In this paper, we have fixed the E_J/E_C ratio to 100, in order to confine the subsystems to the transmon regime. We have considered the value of $\hbar\gamma$, the coupling strength between the subsystems, to be one order of magnitude smaller than the charging energy, to remain in the weak-coupling limit. We took this value to be $0.2E_C$ for further studies. The anharmonicity in the energy spectrum is quantified by the difference in the consecutive excitation energies of this system, given by $E_{12} - E_{01}$, where the energy difference between two eigenstates is denoted by $E_{mn} = E_n - E_m$. The aforementioned parameter space considered in this paper leads the value of the ground-state oscillator energy to be $20\sqrt{2}\hbar$, and the anharmonicity in the consecutive energy levels to be $-E_c$, keeping terms up to first order in the perturbation coefficient $\lambda = E_C/12$. We take the basis $\mathbb{B} = \{|ij\rangle\}$, with i and j running from 0 to 2, as the reference basis for evaluation of the l_1 -norm of quantum coherence in this paper, where $\{|i\rangle\}_{i=0}^2$ forms the three lowest-energy eigenstates of either transmon.

So, in all the succeeding discussions, by ‘‘ l_1 -norm of quantum coherence,’’ we will actually mean the global l_1 -norm of quantum coherence of the composite two-transmon system with respect to the reference basis \mathbb{B} .

From Fig. 1(a), one observes a periodic collapse and revival of entanglement with time when the system is initiated in the pure product state $|00\rangle$. We also study the time dynamics of the global l_1 -norm of quantum coherence, along with the trace distance [94] and fidelity [92–94], of the time-evolved state from the initial one. The trace distance D and fidelity F between two arbitrary states ρ and σ are defined as

$$D(\rho, \sigma) = \frac{1}{2} \|\rho - \sigma\|_1, \quad (9)$$

$$F(\rho, \sigma) = (\text{Tr} \sqrt{\sqrt{\rho} \sigma \sqrt{\rho}})^2. \quad (10)$$

We observe that these quantities also vary in a qualitatively similar fashion like the entanglement, but with different amplitudes, and in some cases with a phase shift of $\pm\pi$.

In Fig. 1(b), we demonstrate the time variation of the l_1 -norm of quantum coherence and trace distance under the same unitary evolution when the system is initially prepared in the $|11\rangle$ state. As in the previous case [Fig. 1(a)], and as it may be expected, oscillatory behavior in time persists. The entanglement generated from the composite initial state $|11\rangle$ changes in a similar manner as the quantum coherence of the same initial state [see Fig. 1(b) blue line], the only difference being the absence of the small ‘‘eddy’’ oscillations present in the coherence dynamics. When we initialize the system with separable states of higher energy, such as $|22\rangle$, we observe a generation of entanglement with very small amplitudes, although the oscillatory nature of this

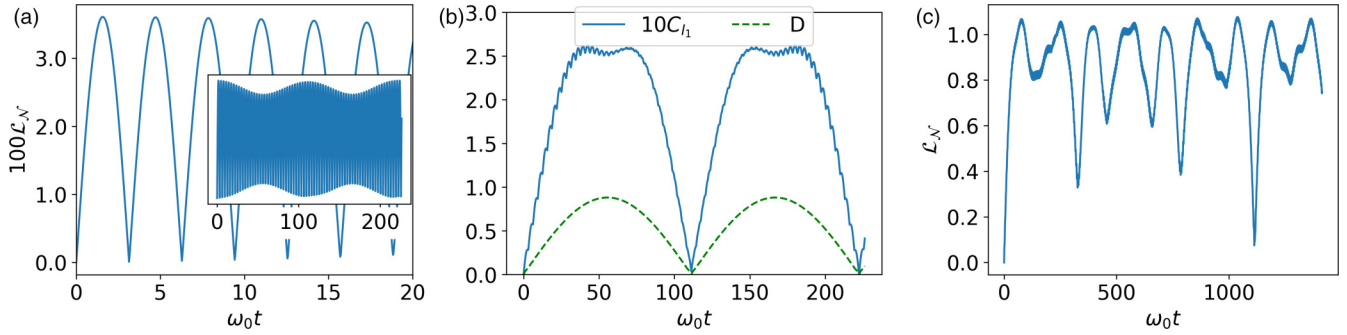


FIG. 1. Time dynamics of quantum resources generated in a pair of coupled transmon qutrits isolated from their surroundings. We plot the variation of the logarithmic negativity with time for the composite system of interacting transmon qutrits described in Eq. (5) in panel (a). The initial state of the system is $|00\rangle$. The long-time behavior of entanglement for this case is presented in the inset. The l_1 -norm of quantum coherence of the system with the initial state $|11\rangle$ is depicted in panel (b) with the blue line. The green dashed line in panel (b) presents the trace distance between the time-evolved state and the initial state $|11\rangle$. Panel (c) describes the time dynamics of logarithmic negativity in the system, when it starts out from the state $|\psi_1\rangle \otimes |\psi_2\rangle$, where $\psi_1 = (|0\rangle + |1\rangle)/\sqrt{2}$ and $\psi_2 = (|0\rangle + |2\rangle)/\sqrt{2}$. The ratio of the Josephson energy to the charging energy for both the subsystems is taken to be $E_J/E_C = 100$. The coupling strength between the subsystems is chosen such that $\gamma = 0.2E_C/\hbar$. The quantities \mathcal{L}_N and C_{l_1} , demonstrated along the vertical axes, are in ebits and cobits, respectively, and the quantity D depicted by the green dashed line in panel (b) is dimensionless. The quantity plotted along the horizontal axes of all the panels and the inset is the dimensionless quantity, $\omega_0 t$.

entanglement generation remains similar with the cases depicted in Figs. 1(a) and 1(b). Also, the quantum coherence generation in this case is qualitatively the same as we obtained for the initial states $|00\rangle$ and $|11\rangle$. Various other initial separable states, e.g., $|++\rangle$, have been considered. The qualitative features remain similar irrespective of the choice of initial separable state. The amplitude profiles of the oscillatory dynamics of entanglement and quantum coherence change in a periodic manner, as can be seen from the inset of Fig. 1(a). Noticeably, the frequency and maximum amplitude of this envelope increase rapidly with increasing coupling strength. See also Fig. 1(c), for the state $|\psi_1\rangle \otimes |\psi_2\rangle$, where $|\psi_1\rangle = (|0\rangle + |1\rangle)/\sqrt{2}$ and $|\psi_2\rangle = (|0\rangle + |2\rangle)/\sqrt{2}$. In this scenario, entanglement again displays oscillatory behavior, but the period of these oscillations is greater than that observed in the cases when the initial states are $|00\rangle$ and $|11\rangle$. In short, the measures of the quantum resources studied in this paper behave in a qualitatively similar fashion under unitary evolution, when the system starts from separable states.

In contrast, entanglement remains almost constant in time when the system starts from the entangled state, $(|01\rangle + |10\rangle)/\sqrt{2}$. We find that this result remains the same for some other entangled states, e.g., $(|12\rangle + |21\rangle)/\sqrt{2}$, as well. However, the global quantum coherence of the system still maintains the oscillatory behavior, which is very similar to the entanglement in Fig. 1(a) for these entangled states.

Therefore, from the observations of the unitary evolution of a pair of coupled transmons, we can infer that one can generate significant quantum resources by a coupled transmon system, when the composite system is isolated from its surroundings. These scenarios are far from the actual situations, as in reality the described transmon qutrits are never isolated, but are connected to other circuit elements as well. These circuit elements along with noncircuit environs can be considered as environments attached to the individual qutrits. Environments may cause substantial adverse effects on the time dynamics of the quantum resources for the system under

consideration. In the succeeding parts of this paper, we will study the effects of environments on the “ideal” coupled-transmons setup.

B. Dynamical equation in presence of Markovian baths

Quantum systems are generally susceptible to environmental effects, and hence it is important to study the influence of environments on the generation of quantum resources in coupled transmon qutrits, if these resources are to be used in real quantum devices. In that spirit, here we consider the system described by the Hamiltonian H_s [see Eq. (5)], in presence of two independent harmonic oscillator baths, separately coupled to the two transmon qutrits locally. As mentioned before, the system-bath coupling is taken to be weak for the validation of Born-Markov approximations [88–91]. The bath Hamiltonians are given by

$$H_{B_i} = \sum_j \hbar \nu_j^i b_j^{\dagger i} b_j^i, \quad (11)$$

for $i = 1$ and 2 . ν_j^i is the frequency of the j th mode of the i th bath. b_j^i ($b_j^{\dagger i}$) is the bosonic annihilation (creation) operator of the i th bath corresponding to the j th mode. The oscillator modes interact with the system through the net content of Cooper pairs across the junction, i.e., the reduced charge (\hat{n}) of the system. This introduces a system-bath interaction of the following form [60]:

$$H_{SB} = \sum_{i=1}^2 \hbar q^i \sum_j g_j^i (\hat{b}_j^{\dagger i} + \hat{b}_j^i), \quad (12)$$

with g_j^i being the coupling constant having the unit of frequency, for tuning the interaction strength between the i th system and j th mode of the i th bath. Here $q^1 = (\sum_{l,m} |l\rangle \langle l| \hat{n}_1 \otimes \mathbb{I}_3 |m\rangle \langle m|)$ and $q^2 = (\sum_{l,m} |l\rangle \langle l| \mathbb{I}_3 \otimes \hat{n}_2 |m\rangle \langle m|)$, i.e., the reduced charge (number of Cooper pairs) operators expressed in the eigenbasis of system-Hamiltonian H_s , and \mathbb{I}_3 is the

identity matrix on the three-dimensional Hilbert space of a transmon qutrit. Hence, the total Hamiltonian of the composite system-bath setup, with a harmonic oscillator bath coupled to each transmon qutrit locally in the circuit, reads

$$H_{\text{total}} = H_s + \sum_{i=1}^2 H_{B_i} + H_{\text{SB}}. \quad (13)$$

In presence of these Markovian bosonic baths, the system undergoes an open-system dynamics governed by the Gorini-Kossakowski-Sudarshan-Lindblad master equation, given by [88–91]

$$\frac{d\rho_s(t)}{dt} = -\frac{i}{\hbar}[H_s, \rho_s(t)] + \sum_{i=1}^2 \mathcal{D}_i[\rho_s(t)]. \quad (14)$$

Here $\rho_s(t)$ is the composite two-transmon state at time t after tracing out the Markovian baths. $\mathcal{D}_i[\rho_s(t)]$ is the dissipative term coming from the interaction between the i th system and the i th bath, presented as

$$\begin{aligned} \mathcal{D}_i(\rho_s(t)) = & \frac{1}{2} \sum_{\omega_{nm} > 0} S_i(\omega_{nm}) [2\Pi_{nm}^i \rho_s(t) \Pi_{nm}^{i\dagger} \\ & - \{\Pi_{nm}^{i\dagger} \Pi_{nm}^i, \rho_s(t)\}] + \frac{1}{2} \sum_{\omega_{nm} > 0} S_i(-\omega_{nm}) \\ & \times [2\Pi_{nm}^{i\dagger} \rho_s(t) \Pi_{nm}^i - \{\Pi_{nm}^i \Pi_{nm}^{i\dagger}, \rho_s(t)\}] \\ & + \frac{1}{2} \sum_n S_i(0) [2\Pi_{nn}^i \rho_s(t) \Pi_{nn}^i \\ & - \{\Pi_{nn}^i \Pi_{nn}^i, \rho_s(t)\}], \end{aligned} \quad (15)$$

where $\omega_{nm} = \omega_m - \omega_n$. Here ω_n denotes the eigenfrequencies of the composite system described by Eq. (5), and Π_{nm}^i are the Lindblad operators, for $i = 1$ and 2 , where $\Pi_{nm}^i = q_{nm}^i |n\rangle\langle m|$ and $q_{nm}^i = \langle n| q^i |m\rangle$. The transition rate, $S_i(\omega)$, turns out to be

$$S_i(\omega) = \frac{J_i(\omega)}{1 - e^{-\hbar\beta_i\omega}}, \quad (16)$$

where $\beta_i = 1/k_B T_i$. Here T_i denotes the absolute temperature of the i th bath and k_B is the Boltzmann constant. $J_i(\omega)$ represents the spectral density function of the harmonic oscillator baths, which we have chosen to be Ohmic, the functional form of which is given by

$$J_i(\omega) = \frac{\kappa_i \omega / \omega_{01}}{[1 + (\omega / \Omega_{c_i})^2]^2}, \quad (17)$$

where $\hbar\omega_{01}$ denotes the energy difference between the first two levels of the composite transmon system described by the Hamiltonian H_s . We fix the algebraic cutoff $\Omega_{c_1} = \Omega_{c_2} = 50\omega_{01}$ in order to keep this cutoff frequency sufficiently large compared to the low-lying energy levels of the system. The relation (17) holds for Ohmic baths with second-order Drude cutoff. κ_i , the spontaneous emission rate in the Lindblad equation, modulates the coupling strength between the i th subsystem and corresponding bath. The system-bath coupling constants are considered to be such that $\kappa_1 = \kappa_2 = \omega_{01}/20$, for subsequent computations throughout this paper, so that the Markovian approximations remain valid. As a result, the

system-bath interaction belongs to the weak-coupling regime: $S(\omega_{nm}) \ll |\omega_{nm}|$ [88–91].

C. Resource generation in presence of Markovian baths

In Fig. 2, we describe the time variations of logarithmic negativity and l_1 -norm of quantum coherence of the two-transmon system considered in Eq. (5), initially starting from separable states. We observe that the entanglement between the two qutrits of the system, as well as the global quantum coherence of the system, initially increases quickly to a maximum value and then decays to a steady value in an oscillatory manner with decreasing amplitudes of oscillations. These intermediate oscillations between the maximum and the saturated value are more prominent when the system is initialized in the $|00\rangle$ state than the case when the system starts from an excited state $|11\rangle$ [Figs. 2(a) and 2(b)]. When initiating both qutrits in their highest excited states, i.e., $|22\rangle$, we observe that the amplitude of the generated entanglement is very small and quantum coherence exhibits similar behavior as in the cases of $|00\rangle$ and $|11\rangle$. For the initial state $|\psi_1\rangle \otimes |\psi_2\rangle$, as illustrated in Fig. 2(c), the amplitude of quantum entanglement diminishes when subjected to Markovian baths, demonstrating a similar behavior to that of the $|00\rangle$ and $|11\rangle$ states. However, in contrast to the cases initiated with the $|00\rangle$ and $|11\rangle$ states, here quantum coherence begins with a nonzero value and rapidly diminishes without any noticeable intermediate revival, following an exponential decay pattern.

This behavior is, however, distinctly different when the system is initially prepared in an entangled state. When we start from the entangled state $(|01\rangle + |10\rangle)/\sqrt{2}$ for the each subsystem, the entanglement and quantum coherence decay exponentially. See Fig. 3. We also found the same behavior for the state $(|12\rangle + |21\rangle)/\sqrt{2}$.

In absence of any interaction in the system Hamiltonian, i.e., for $\gamma = 0$, the system only goes through decoherence. As a result, an initial system density matrix with nonzero quantum coherence decays to a zero resource state very soon, and a separable state remains separable. In contrast, the system studied in this paper has a nonlocal interaction term H_{int} in the system Hamiltonian, arising due to the interaction between the transmon components present in the system. This nonlocal interaction term works in favor of continuously feeding quantum resources into the system, whereas quantum resources leak out into the environment simultaneously, due to the Markovian baths. These two mechanisms act in opposition. For small initial times, the quantum resources exhibit oscillatory nature as in the unitary case (see Fig. 1) since the decoherence due to the baths is very small then, which gradually build ups to a substantial value. In the long-time limit, the competition between these two mechanisms leads the system towards a steady state. Consequently, the quantum resources considered in this paper attain nonzero steady values as well.

The following comment is in order here. The oscillatory behavior seen, e.g., in entanglement decay in Fig. 2(a) is reminiscent of the behavior of entanglement for local non-Markovian baths in presence of intertransmon coupling (see, e.g., [95] and references therein). It therefore seems that the typical non-Markovian phenomenon can be mimicked by Markovian baths in presence of intrasystem interactions.

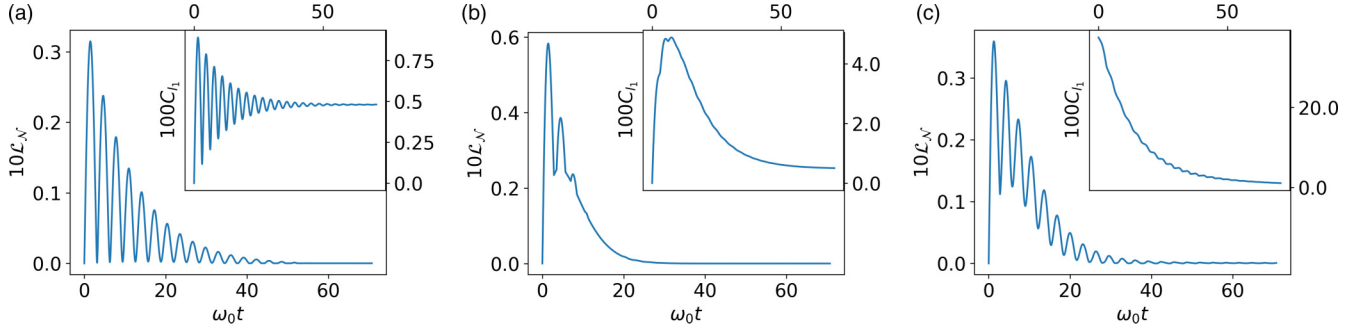


FIG. 2. Mimicking non-Markovianity: Time dynamics of entanglement and quantum coherence for initial separable states of coupled transmon qutrits locally immersed in Markovian bosonic baths. Here we demonstrate the logarithmic negativity between the qutrits of the system in the main figures and the global l_1 -norms of quantum coherence of the system in the insets for the initial states (a) $\rho_s(0) = |00\rangle\langle 00|$, (b) $\rho_s(0) = |11\rangle\langle 11|$, and (c) $\rho_s(0) = |\psi_1\rangle\langle\psi_1| \otimes |\psi_2\rangle\langle\psi_2|$, where $|\psi_1\rangle = (|0\rangle + |1\rangle)/\sqrt{2}$ and $|\psi_2\rangle = (|0\rangle + |2\rangle)/\sqrt{2}$. The system parameters are the same as in Fig. 1. We have taken $\kappa_1 = \kappa_2 = \omega_{01}/20$, and the temperatures of the baths are chosen to be such that $\beta_1 = \beta_2 = 5/(\hbar\omega_{01})$. The quantities $\mathcal{L}_{\mathcal{N}}$ and C_{l_1} plotted along the vertical axes are in ebits and cobits, respectively. The quantity presented along the horizontal axes in all panels and insets is the dimensionless quantity, $\omega_0 t$.

D. Resource generation in presence of local baths with different temperatures

In the depiction of Figs. 2 and 3, we have focused on scenarios in which the two transmon qutrits are individually submerged in two distinct thermal baths, both operating at the same temperature. Under the condition that the dynamics of the system adhere strictly to Markovian approximations [88–91], and the contribution of three- and higher-body interaction terms between the transmons and the bath is negligible, these two local thermal baths, despite their separate existence, effectively function as a single heat bath connected to both the transmons. The possibility of bath mediated interaction in presence of a common bath can be ignored within the ap-

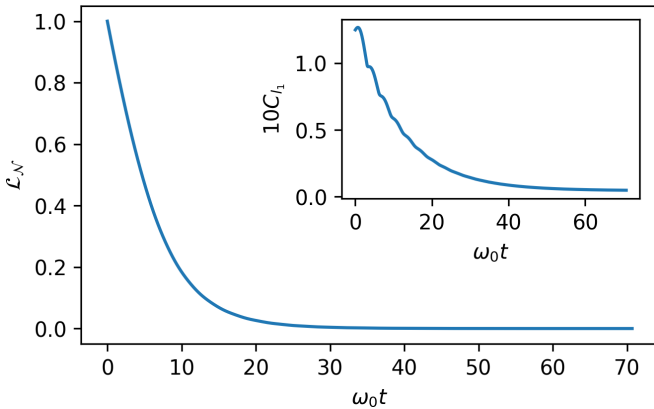


FIG. 3. Time dynamics of entanglement and quantum coherence for an initial entangled state of the coupled transmon qutrits locally immersed in Markovian bosonic baths. Here we depict the time evolution of logarithmic negativity between the two qutrits (in the main figure) and the global l_1 -norm of quantum coherence of the system (in the inset) in presence of Markovian baths for the initial state $\rho_s(0) = |\psi_s(0)\rangle\langle\psi_s(0)|$, with $|\psi_s(0)\rangle = (|01\rangle + |10\rangle)/\sqrt{2}$. All other considerations are the same as in Figs. 1 and 2. The quantities $\mathcal{L}_{\mathcal{N}}$ and C_{l_1} plotted along the vertical axes are in ebits and cobits, respectively. The quantity presented along the horizontal axes is dimensionless.

proximate evolution considered. The situation can be altered to explore the impacts of two distinct local baths by adjusting their temperatures accordingly. As depicted in Fig. 4, employing baths at different temperatures results in a significantly faster decay of bipartite entanglement, in comparison to using baths at the same temperature, when both transmon qutrits initially start in a separable state originating from their respective ground states. See Fig. 4(a). The same figure also highlights the correlation that a greater temperature difference between the local baths leads to a faster decay in bipartite entanglement between the two transmons. It is essential to note that the rate of decay of entanglement depends upon the chosen initial state of the system. See Figs. 4(a)–4(d). Nonetheless, as exemplified by the states presented in the four panels of Fig. 4, it is apparent that the entanglement generating capacity of the system is compromised in the presence of local baths at different temperatures. Note that quantum coherence also exhibits a qualitatively similar behavior to entanglement in response to changes in bath temperatures. Hence, to maximize the generated entanglement and quantum coherence of the capacitively coupled two-transmon system, we carry this study forward with the transmons connected to same temperature Markovian baths.

E. Dependence of resource generation on capacitive coupling strength

The capacitive coupling between the transmon qutrits can be implemented in real experimental setups conveniently. The experimental setup of the system studied in our paper can be built with two Josephson junctions of Josephson energy E_J , shunted with two capacitors C_1 and C_2 , yielding a charging energy E_C in the individual circuits. When a capacitor with capacitance C_g is placed between the voltage nodes (with voltages V_1 and V_2) of the two participating transmon circuits, we obtain the capacitive coupling. This yields a nonlocal interaction term in the Hamiltonian of the form [12]

$$H_I = C_g V_1 V_2.$$

Circuit quantization in the limit of $C_g \ll C_1, C_2$ yields an interaction term in the form of Eq. (4), where we can express

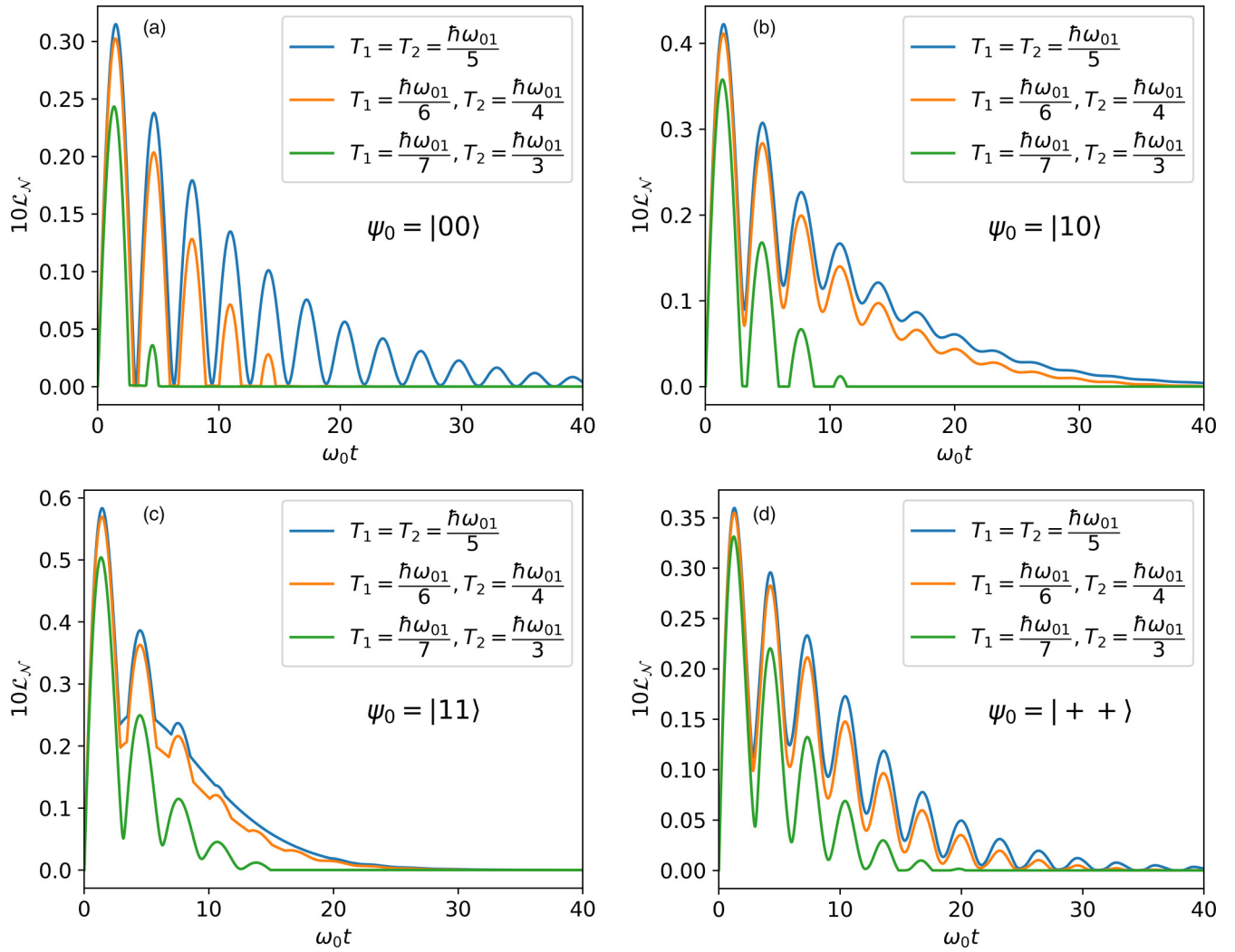


FIG. 4. Comparison of entanglement dynamics between two capacitively coupled transmon qutrits in contact with local baths at same or different temperatures, for different initial states $\rho_0 = |\psi_0\rangle\langle\psi_0|$. All other considerations are the same as in Figs. 1 and 2. The corresponding bath temperatures are specified in the legends, wherein $\hbar\omega_{01}$ is the energy required for any of the transmons to make a transition from the ground state to the first excited state. Logarithmic negativity (\mathcal{L}_N) plotted along the vertical axes is in the unit of ebits, and the quantities depicted along the horizontal axes are dimensionless.

the interaction parameter γ in terms of the circuit elements as

$$\hbar\gamma = 4e^2 \frac{C_g}{C_1 C_2}. \quad (18)$$

The quantum resources exhibit an oscillatory nature and reach a maximum value during the oscillation for the unitary evolution of the system described in Sec. IV A (see Fig. 1). We observe that these maximum values of the bipartite entanglement and the global quantum coherence in such an isolated system of two capacitively coupled transmon qutrits increase with increasing strength of the interaction γ . The case for logarithmic negativity is depicted in Fig. 5 for increasing values of γ . The global l_1 -norm of quantum coherence of the system also varies similarly with the transmon-transmon coupling strength γ .

We now scrutinize the dependence of resource generation on the coupling strength γ for the coupled transmons setup immersed in Markovian bosonic baths, described in the preceding subsection. In Figs. 6(a) and 6(b) we depict the

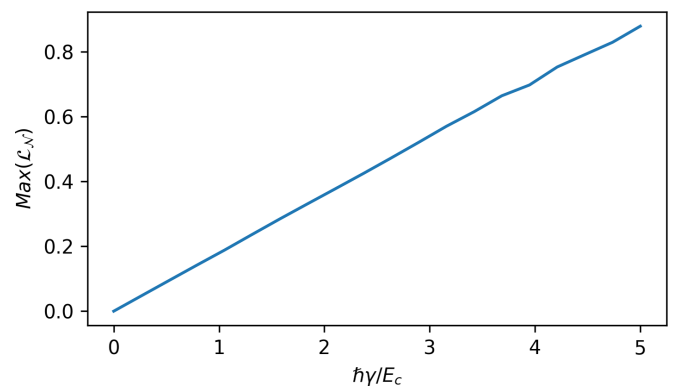


FIG. 5. Variation of maximum entanglement with varying capacitive coupling strength under unitary evolution, described by the Hamiltonian in Eq. (5). The initial state is chosen to be the separable state $\rho_s(0) = |00\rangle\langle 00|$. All other considerations are the same as in Fig. 1. The quantity plotted along the vertical axis is in ebits and the same plotted against the horizontal axis is dimensionless.

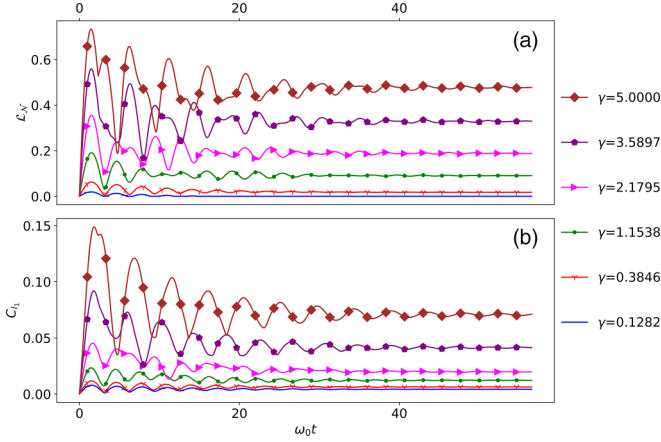


FIG. 6. Quantum resource generation in coupled transmons for different values of interaction strength between two capacitively coupled transmon qutrits, both immersed in bosonic baths, as described by Eq. (13). Panel (a) describes the time variation of logarithmic negativity in the system, and panel (b) describes the time evolution of the l_1 -norm of quantum coherence of the system. The initial state is taken as $|\psi_s(0)\rangle = |00\rangle$, which has vanishing amounts of both quantum resources. The values of the interaction strength γ are given in the legend in units of E_c/\hbar . All other considerations are the same as in Figs. 1 and 2. The quantities \mathcal{L}_N and C_l plotted along the vertical axes are in ebits and cobits, respectively. The quantity presented along the horizontal axes is dimensionless.

time dynamics of logarithmic negativity and the l_1 -norm of quantum coherence, respectively, for different strengths of the capacitive coupling between the two transmon qutrits. Here we vary the interaction strength in the regime so that the circuit quantization yielding the interaction term in the form mentioned in Eq. (18) remains valid. As can be seen from Fig. 6, the maximum values of bipartite entanglement and quantum coherence, along with the long-time steady-state values of the same, increase with stronger coupling between the subsystems, and finally sustain a nonzero finite value. This demonstrates that for initial states with zero quantum resources and even for small nonzero interactions in the form of Eq. (4), not only the maximum quantum resources in the system studied increase, but the decoherence time increases profoundly. This result shows that the ability of creation of coupled transmon circuits with tunable charge-charge interaction promises us control over the decoherence time of the system, which translates to potentially improved practical implementations and utilizations of the described system in future. Note that we cannot increase the self-generated quantum resources indefinitely by choosing a higher value of γ . In the range from zero to one-fifth of the ground-state energy (of the isolated coupled transmon qutrits) of γ , the quantum resources increase almost linearly with the increase of γ . Beyond this weak-coupling (between the subsystems) regime, the rate of increase of maximum self-generated quantum resources with increase in γ starts to slow down and approaches saturation to a finite value, for both the ideal coupled transmon setup isolated from the environment as well as in presence of Markovian environments. In our depiction, we have not studied that region of γ , as the treatment used here is exclusively suitable only for the weak-coupling regime of the

system. In Figs. 5 and 6 we have shown the cases for the initial state $|\psi_s(0)\rangle = |0\rangle$, but we have also studied the case for some more paradigmatic initial separable states. The results are qualitatively similar.

V. OPTIMAL ENTANGLEMENT GENERATION WITH UNENTANGLED INITIAL STATES

In the previous sections, we have witnessed that two interacting transmon qutrits can generate quantum resources even in presence of decoherence effects of the environment and can sustain a substantial amount of the same for a finite duration of time, when we start off from certain zero resource states. We have also described that if we start from the states of the system with nonzero resources, they may be incapable of generating significant quantum resources. It is also plausible that for generating a resource, we will mostly encounter situations where we are required to begin with an insignificant amount of the same resource. This leads us to search for the optimal generation of a resource when we start off from a zero quantum resource state. In connection to this, here we define the entanglement generation power of coupled transmon systems with initial separable states.

The definition depends on two aspects: (a) the maximum value of the entanglement the system can self-generate, and (b) the timescale over which the system can retain a substantial value of this entanglement. Let the maximum generated logarithmic negativity for a separable initial two-qutrit state be \mathcal{L}_N^{\max} . We set the threshold for defining the timescale over which the generated entanglement remains substantial to half of the maximum generated entanglement, $\frac{1}{2}\mathcal{L}_N^{\max}$, beyond which the entanglement is assumed to be too small to be useful and hence not taken into account. This reminds one of the correction of using full width (duration) at half maximum measure resolution in signal processing and other fields. Therefore, the entanglement generation power of a coupled transmon system, as a function of its initial state, can be given by

$$\mathcal{E}(\rho_s^0) = \sum_n \int_{t_{n-}}^{t_{n+}} \mathcal{L}_N(\rho_s^0) dt. \quad (19)$$

Here t_{n-} to t_{n+} is the time interval during which the system can generate entanglement $\geq \mathcal{L}_N^{\max}/2$ under the n th peak, and we are taking the summation over all such time intervals to measure entanglement generating power of the system.

In search of the initial state providing the maximum generation of bipartite entanglement in the system described, we optimize the quantity and define the optimal entanglement generating power of the system as

$$\mathcal{E}_{\text{opt}} = \max_{\rho_s^0 \in \mathcal{S}} \mathcal{E}(\rho_s^0), \quad (20)$$

with \mathcal{S} being the set of all pure or mixed product states on the $\mathbb{C}^3 \otimes \mathbb{C}^3$ Hilbert space.

In Fig. 7, we depict the logarithmic negativity for the optimal initial state $\rho_{s_{\text{opt}}}^0$. The form of $\rho_{s_{\text{opt}}}^0$ is described in the caption of the same figure. For this optimal state, we get the optimal entanglement generating power, $\mathcal{E}_{\text{opt}} \simeq 0.01433$ ebits. The optimization is performed by separate Haar-uniform generations of 2×10^3 pure product and mixed product states.

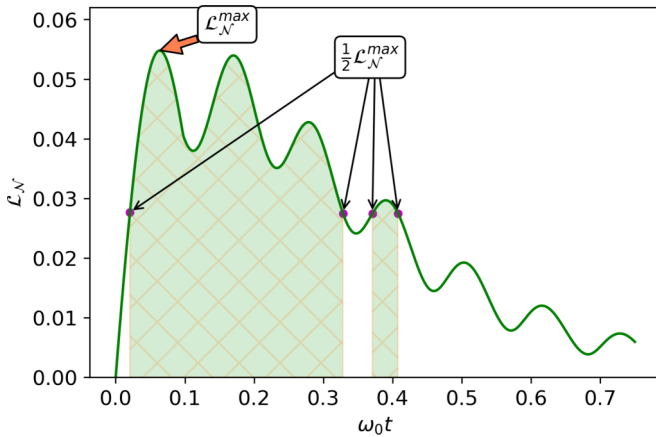


FIG. 7. Maximum entanglement generating power of coupled transmons. Here we plot the logarithmic negativity against time for the optimal initial state ρ_{opt}^0 . The optimal state is found to be $\rho_{\text{opt}}^0 = |\psi_0^1\rangle\langle\psi_0^1| \otimes |\psi_0^2\rangle\langle\psi_0^2|$ with $|\psi_0^1\rangle = (-0.256 - 0.492i)|0\rangle + (-0.479 + 0.680i)|1\rangle$ and $|\psi_0^2\rangle = (-0.395 + 0.392i)|0\rangle + (-0.768 - 0.316i)|1\rangle$. All other considerations are the same as in Figs. 1 and 2. The quantity plotted along the vertical axis is in ebits and the same plotted along the horizontal axis is dimensionless.

VI. CONCLUSION

We have studied a system of two transmons, coupled through their charge degrees of freedom. We have taken into account up to the second excited state of the individual subsystems, appealing to the typical decoherence times of transmon systems, with very small values of the charging energy of Cooper pairs, compared to the Josephson energy. Transmons, coupled through a capacitor of capacitance very small compared to that of the individual transmon circuits, allows us to write the total Hamiltonian in a compact form through circuit quantization, thereby providing us with the scope of systematic studies of such realistic systems. The obtained results reported in this paper are drawn upon the assumption that the transmons are immersed in independent bosonic baths, within the Markovian limit.

It turns out that such a system can attain a substantial value of entanglement and quantum coherence, even when it starts from states with zero resource. We noticed that a larger temperature difference between the two local baths speeds up the decay of quantum resources in the two-transmon system. In the weakly interacting limit, we have also found that for interaction strengths that are small compared to other energy scales in the system, this self-generated resource in the system increases almost linearly with increasing coupling strength and the long-time value of entanglement and global quantum coherence of the system maintains a significant value. Without the nonlocal interaction term between the two transmons, entanglement in the system would only decay due to loss of information to the Markovian baths. However, the interaction present in between the subsystems opposes this decay by feeding resources into the system. We found that even for relatively small nonzero interactions in the system, the entanglement of the composite system does not entirely vanish. The competition between the pumping of the resource by the nonlocal interaction and the loss of the same due to the interaction with the baths results in a sustenance of a stable value of entanglement between the transmons. The nonmonotonic oscillation, in time, of the intertransmon entanglement is reminiscent of backflow effects in non-Markovian environments in absence of intrasystem coupling. We also define the optimal entanglement generating power for a coupled transmon system and obtain the best two-qutrit input state, initialized in the corresponding qubit subspaces, which can offer the optimal entanglement generating power of the system under consideration.

ACKNOWLEDGMENTS

The research of T.R. and A.G. was supported in part by the “INFOSYS scholarship for senior students.” D.R. acknowledges support from Science and Engineering Research Board (SERB), Department of Science and Technology (DST), under the sanction No. SRG/2021/002316-G. We also acknowledge partial support from the Department of Science and Technology, Government of India through QuEST Grant No. DST/ICPS/QUST/Theme-3/2019/120.

-
- [1] D. Deutsch and R. Jozsa, Rapid solution of problems by quantum computation, *Proc. R. Soc. A* **439**, 553 (1992).
 - [2] P. W. Shor, Polynomial-time algorithms for prime factorization and discrete logarithms on a quantum computer, *SIAM J. Sci. Stat. Comput.* **26**, 1484 (1997).
 - [3] L. K. Grover, Quantum mechanics helps in searching for a needle in a haystack, *Phys. Rev. Lett.* **79**, 325 (1997).
 - [4] N. Gisin, G. Ribordy, W. Tittel, and H. Zbinden, Quantum cryptography, *Rev. Mod. Phys.* **74**, 145 (2002).
 - [5] D. Leibfried, R. Blatt, C. Monroe, and D. Wineland, Quantum dynamics of single trapped ions, *Rev. Mod. Phys.* **75**, 281 (2003).
 - [6] R. Blatt and C. F. Roos, Quantum simulations with trapped ions, *Nat. Phys.* **8**, 277 (2012).
 - [7] J. You and F. Nori, Superconducting circuits and quantum information, *Phys. Today* **58**(11), 42 (2005).
 - [8] J. You and F. Nori, Atomic physics and quantum optics using superconducting circuits, *Nature (London)* **474**, 589 (2011).
 - [9] P. Nation, J. Johansson, M. Blencowe, and F. Nori, Colloquium: Stimulating uncertainty: Amplifying the quantum vacuum with superconducting circuits, *Rev. Mod. Phys.* **84**, 1 (2012).
 - [10] G. Wendin, Quantum information processing with superconducting circuits: A review, *Rep. Prog. Phys.* **80**, 106001 (2017).
 - [11] X. Gu, A. F. Kockum, A. Miranowicz, Y.-X. Liu, and F. Nori, Microwave photonics with superconducting quantum circuits, *Phys. Rep.* **718–719**, 1 (2017).
 - [12] P. Krantz, M. Kjaergaard, F. Yan, T. P. Orlando, S. Gustavsson, and W. D. Oliver, A quantum engineer’s guide to superconducting qubits, *Appl. Phys. Rev.* **6**, 021318 (2019).
 - [13] A. F. Kockum and F. Nori, Quantum bits with Josephson junctions, in *Fundamentals and Frontiers of the Josephson Effect* (Springer, New York, 2019), pp. 703–741.

- [14] M. Kjaergaard, M. E. Schwartz, J. Braumüller, P. Krantz, J. I.-J. Wang, S. Gustavsson, and W. D. Oliver, Superconducting qubits: Current state of play, *Annu. Rev. Condens. Matter Phys.* **11**, 369 (2020).
- [15] X.-L. Wang, L.-K. Chen, W. Li, H.-L. Huang, C. Liu, C. Chen, Y.-H. Luo, Z.-E. Su, D. Wu, Z.-D. Li, H. Lu, Y. Hu, X. Jiang, C.-Z. Peng, L. Li, N.-L. Liu, Y.-A. Chen, C.-Y. Lu, and J.-W. Pan, Experimental ten-photon entanglement, *Phys. Rev. Lett.* **117**, 210502 (2016).
- [16] H.-L. Huang, Q. Zhao, X. Ma, C. Liu, Z.-E. Su, X.-L. Wang, L. Li, N.-L. Liu, B. C. Sanders, C.-Y. Lu, and J.-W. Pan, Experimental blind quantum computing for a classical client, *Phys. Rev. Lett.* **119**, 050503 (2017).
- [17] X.-L. Wang, Y.-H. Luo, H.-L. Huang, M.-C. Chen, Z.-E. Su, C. Liu, C. Chen, W. Li, Y.-Q. Fang, X. Jiang, J. Zhang, L. Li, N.-L. Liu, C.-Y. Lu, and J.-W. Pan, 18-qubit entanglement with six photons' three degrees of freedom, *Phys. Rev. Lett.* **120**, 260502 (2018).
- [18] H.-L. Huang, X.-L. Wang, P. P. Rohde, Y.-H. Luo, Y.-W. Zhao, C. Liu, L. Li, N.-L. Liu, C.-Y. Lu, and J.-W. Pan, Demonstration of topological data analysis on a quantum processor, *Optica* **5**, 193 (2018).
- [19] H. Wang, J. Qin, X. Ding, M.-C. Chen, S. Chen, X. You, Y.-M. He, X. Jiang, L. You, Z. Wang, C. Schneider, J. J. Renema, S. Höfling, C.-Y. Lu, and J.-W. Pan, Boson Sampling with 20 input photons and a 60-mode interferometer in a 10^{14} -dimensional hilbert space, *Phys. Rev. Lett.* **123**, 250503 (2019).
- [20] B. E. Kane, A silicon-based nuclear spin quantum computer, *Nature (London)* **393**, 133 (1998).
- [21] Y. He, S. K. Gorman, D. Keith, L. Kranz, J. G. Keizer, and M. Y. Simmons, A two-qubit gate between phosphorus donor electrons in silicon, *Nature (London)* **571**, 371 (2019).
- [22] Y. Makhlin, G. Schön, and A. Shnirman, Quantum-state engineering with Josephson-junction devices, *Rev. Mod. Phys.* **73**, 357 (2001).
- [23] M. H. Devoret and J. M. Martinis, in *Quantum Entanglement and Information Processing (Les Houches Session LXXIX)*, edited by J.-M. Raimond, J. Dalibard, and D. Esteve (Elsevier, New York, 2003).
- [24] M. H. Devoret, A. Wallraff, and J. M. Martinis, Superconducting qubits: A short review, [arXiv:cond-mat/0411174](https://arxiv.org/abs/cond-mat/0411174).
- [25] F. Arute *et al.*, Quantum supremacy using a programmable superconducting processor, *Nature (London)* **574**, 505 (2019).
- [26] V. Bouchiat, D. Vion, P. Joyez, D. Esteve, and M. H. Devoret, Quantum coherence with a single Cooper pair, *Phys. Scr.* **1998**, 165 (1998).
- [27] Y. Nakamura, Yu. A. Pashkin, and J. S. Tsai, Coherent control of macroscopic quantum states in a single-Cooper-pair box, *Nature (London)* **398**, 786 (1999).
- [28] J. R. Friedman, V. Patel, W. Chen, S. K. Tolpygo, and J. E. Lukens, Quantum superposition of distinct macroscopic states, *Nature (London)* **406**, 43 (2000).
- [29] C. H. van der Wal, A. C. J. ter Haar, F. K. Wilhelm, R. N. Schouten, C. J. P. M. Harmans, T. P. Orlando, S. Lloyd, and J. E. Mooij, Quantum superposition of macroscopic persistent-current states, *Science* **290**, 773 (2000).
- [30] J. M. Martinis, S. Nam, J. Aumentado, and C. Urbina, Rabi oscillations in a large Josephson-junction qubit, *Phys. Rev. Lett.* **89**, 117901 (2002).
- [31] J. Koch, T. M. Yu, J. Gambetta, A. A. Houck, D. I. Schuster, J. Majer, A. Blais, M. H. Devoret, S. M. Girvin, and R. J. Schoelkopf, Charge-insensitive qubit design derived from the Cooper pair box, *Phys. Rev. A* **76**, 042319 (2007).
- [32] B. D. Josephson, Possible new effects in superconductive tunnelling, *Phys. Lett.* **7**, 251 (1962).
- [33] A. Blais, J. Gambetta, A. Wallraff, D. I. Schuster, S. M. Girvin, M. H. Devoret, and R. J. Schoelkopf, Quantum-information processing with circuit quantum electrodynamics, *Phys. Rev. A* **75**, 032329 (2007).
- [34] X. Pan, Y. Zhou, H. Yuan, L. Nie, W. Wei, L. Zhang, J. Li, S. Liu, Z. H. Jiang, G. Catelani, L. Hu, F. Yan, and D. Yu, Engineering superconducting qubits to reduce quasiparticles and charge noise, *Nat. Commun.* **13**, 7196 (2022).
- [35] A. Calzona and M. Carrega, Multi-mode architectures for noise-resilient superconducting qubits, *Supercond. Sci. Technol.* **36**, 023001 (2023).
- [36] G. Ithier, E. Collin, P. Joyez, P. J. Meeson, D. Vion, D. Esteve, F. Chiarello, A. Shnirman, Y. Makhlin, J. Schrieffer, and G. Schön, Decoherence in a superconducting quantum bit circuit, *Phys. Rev. B* **72**, 134519 (2005).
- [37] A. Cottet, Ph.D. thesis, Université Paris VI, 2002.
- [38] A. A. Houck, J. Koch, M. H. Devoret, S. M. Girvin, and R. J. Schoelkopf, Life after charge noise: recent results with transmon qubits, *Quantum Inf. Proc.* **8**, 105 (2009).
- [39] S. Novikov, J. E. Robinson, Z. K. Keane, B. Suri, F. C. Wellstood, and B. S. Palmer, Autler-Townes splitting in a three-dimensional transmon superconducting qubit, *Phys. Rev. B* **88**, 060503(R) (2013).
- [40] M. J. Peterer, S. J. Bader, X. Jin, F. Yan, A. Kamal, T. J. Gudmundsen, P. J. Leek, T. P. Orlando, W. D. Oliver, and S. Gustavsson, Coherence and decay of higher energy levels of a superconducting transmon qubit, *Phys. Rev. Lett.* **114**, 010501 (2015).
- [41] Y. Hu, Y. Song, and L. Duan, Quantum interface between a transmon qubit and spins of nitrogen-vacancy centers, *Phys. Rev. A* **96**, 062301 (2017).
- [42] F. Luthi, T. Stavenga, O. W. Enzing, A. Bruno, C. Dickel, N. K. Langford, M. A. Rol, T. S. Jespersen, J. Nygård, P. Krogstrup, and L. DiCarlo, Evolution of nanowire transmon qubits and their coherence in a magnetic field, *Phys. Rev. Lett.* **120**, 100502 (2018).
- [43] A. D. Patterson, J. Rahamim, T. Tsunoda, P. A. Spring, S. Jebari, K. Ratter, M. Mergenthaler, G. Tancredi, B. Vlastakis, M. Esposito, and P. J. Leek, Calibration of a cross-resonance two-qubit gate between directly coupled transmons, *Phys. Rev. Appl.* **12**, 064013 (2019).
- [44] A. P. M. Place, L. V. H. Rodgers, P. Mundada, B. M. Smitham, M. Fitzpatrick, Z. Leng, A. Premkumar, J. Bryon, A. Vrajitoarea, S. Sussman, G. Cheng, T. Madhavan, H. K. Babla, X. H. Le, Y. Gang, B. Jäck, A. Gyenis, N. Yao, R. J. Cava, N. P. de Leon and A. A. Houck, New material platform for superconducting transmon qubits with coherence times exceeding 0.3 milliseconds, *Nat. Commun.* **12**, 1779 (2021).
- [45] A. Antony, M. V. Gustafsson, G. J. Ribeill, M. Ware, A. Rajendran, L. C. G. Govia, T. A. Ohki, T. Taniguchi, K. Watanabe, J. Hone, and K. C. Fong, Miniaturizing transmon qubits using van der Waals materials, *Nano Lett.* **21**, 10122 (2021).

- [46] X. Li *et al.*, Vacuum-gap transmon qubits realized using flip-chip technology, *Appl. Phys. Lett.* **119**, 184003 (2021).
- [47] C. Wang *et al.*, Transmon qubit with relaxation time exceeding 0.5 milliseconds, *npj Quantum Inf.* **8**, 3 (2022).
- [48] J. Krause, C. Dickel, E. Vaal, M. Vielmetter, J. Feng, R. Bounds, G. Catelani, J. M. Fink, and Y. Ando, Magnetic field resilience of three-dimensional transmons with thin-film Al/AIO_x/Al Josephson junctions approaching 1 T, *Phys. Rev. Appl.* **17**, 034032 (2022).
- [49] A. Hertel *et al.*, Gate-tunable transmon using selective-area-grown superconductor-semiconductor hybrid structures on silicon, *Phys. Rev. Appl.* **18**, 034042 (2022).
- [50] S. Majumder, T. Bera, R. Suresh, and V. Singh, A fast tunable 3D-transmon architecture for superconducting qubit-based hybrid devices, *J. Low Temp. Phys.* **207**, 210 (2022).
- [51] M. Zemlicka, E. Redchenko, M. Peruzzo, F. Hassani, A. Trioni, S. Barzanjeh, and J. M. Fink, Compact vacuum gap transmon qubits: Selective and sensitive probes for superconductor surface losses, [arXiv:2206.14104](https://arxiv.org/abs/2206.14104).
- [52] R. Horodecki, P. Horodecki, M. Horodecki, and K. Horodecki, Quantum entanglement, *Rev. Mod. Phys.* **81**, 865 (2009).
- [53] O. Gühne and G. Tóth, Entanglement detection, *Phys. Rep.* **474**, 1 (2009).
- [54] S. Das, T. Chanda, M. Lewenstein, A. Sanpera, A. Sen(De), and U. Sen, The separability versus entanglement problem, in *Quantum Information: From Foundations to Quantum Technology Applications*, 2nd ed., edited by D. Bruß and G. Leuchs (Wiley, New York, 2019).
- [55] J. Åberg, Quantifying superposition, [arXiv:quant-ph/0612146](https://arxiv.org/abs/quant-ph/0612146).
- [56] T. Baumgratz, M. Cramer, and M. B. Plenio, Quantifying coherence, *Phys. Rev. Lett.* **113**, 140401 (2014).
- [57] A. Winter and D. Yang, Operational resource theory of coherence, *Phys. Rev. Lett.* **116**, 120404 (2016).
- [58] A. Streltsov, G. Adesso, and M. B. Plenio, Colloquium: Quantum coherence as a resource, *Rev. Mod. Phys.* **89**, 041003 (2017).
- [59] J. Yang, É. Jussiau, C. Elouard, K. Le Hur, and A. N. Jordan, Quantum system dynamics with a weakly nonlinear Josephson junction bath, *Phys. Rev. B* **103**, 085402 (2021).
- [60] J. Tuorila, J. Stockburger, T. Ala-Nissila, J. Ankerhold, and M. Möttönen, System-environment correlations in qubit initialization and control, *Phys. Rev. Res.* **1**, 013004 (2019).
- [61] A. P. Babu, J. Tuorila, and T. Ala-Nissila, State leakage during fast decay and control of a superconducting transmon qubit, *npj Quantum Inf.* **7**, 30 (2021).
- [62] A. D'Arrigo and E. Paladino, Optimal operating conditions of an entangling two-transmon gate, *New J. Phys.* **14**, 053035 (2012).
- [63] C. Ohm and F. Hassler, Measurement-induced entanglement of two transmon qubits by a single photon, *New J. Phys.* **19**, 053018 (2017).
- [64] X.-H. Deng, E. Barnes, and S. E. Economou, Robustness of error-suppressing entangling gates in cavity-coupled transmon qubits, *Phys. Rev. B* **96**, 035441 (2017).
- [65] C. Dickel, J. J. Wesdorp, N. K. Langford, S. Peiter, R. Sagastizabal, A. Bruno, B. Criger, F. Motzoi, and L. DiCarlo, Chip-to-chip entanglement of transmon qubits using engineered measurement fields, *Phys. Rev. B* **97**, 064508 (2018).
- [66] X.-M. Ye, Z.-F. Zheng, D.-M. Lu, and C.-P. Yang, Circuit QED: Generation of two-transmon-qutrit entangled states via resonant interaction, *Quantum Inf. Proc.* **17**, 99 (2018).
- [67] A. Katarbwa and M. R. Geller, Measurement of GHZ and cluster state entanglement monotones in transmon qubits, [arXiv:1808.05203](https://arxiv.org/abs/1808.05203).
- [68] T. Hurant and D. D. Stancil, Asymmetry of CNOT gate operation in superconducting transmon quantum processors using cross-resonance entangling, [arXiv:2009.01333](https://arxiv.org/abs/2009.01333).
- [69] A. Salmanoglu, Entanglement engineering by transmon qubit in a circuit QED, [arXiv:2109.00316](https://arxiv.org/abs/2109.00316).
- [70] A. Cervera-Lierta, M. Krenn, A. Aspuru-Guzik, and A. Galda, Experimental high-dimensional Greenberger-Horne-Zeilinger entanglement with superconducting transmon qutrits, *Phys. Rev. Appl.* **17**, 024062 (2022).
- [71] A. Maiani, M. Kjaergaard, and C. Schrade, Entangling transmons with low-frequency protected superconducting qubits, *PRX Quantum* **3**, 030329 (2022).
- [72] J. M. Martinis, K. B. Cooper, R. McDermott, M. Steffen, Markus Ansmann, K. D. Osborn, K. Cicak, S. Oh, D. P. Pappas, R. W. Simmonds, and C. C. Yu, Decoherence in Josephson qubits from dielectric loss, *Phys. Rev. Lett.* **95**, 210503 (2005).
- [73] J. A. Schreier, A. A. Houck, J. Koch, D. I. Schuster, B. R. Johnson, J. M. Chow, J. M. Gambetta, J. Majer, L. Frunzio, M. H. Devoret, S. M. Girvin, and R. J. Schoelkopf, Suppressing charge noise decoherence in superconducting charge qubits, *Phys. Rev. B* **77**, 180502(R) (2008).
- [74] S. M. Girvin, M. H. Devoret and R. J. Schoelkopf, Circuit QED and engineering charge-based superconducting qubits, *Phys. Scr.* **2009**, 014012 (2009).
- [75] S. E. Nigg, H. Paik, B. Vlastakis, G. Kirchmair, S. Shankar, L. Frunzio, M. H. Devoret, R. J. Schoelkopf, and S. M. Girvin, Black-box superconducting circuit quantization, *Phys. Rev. Lett.* **108**, 240502 (2012).
- [76] M. H. Devoret, in *Quantum Fluctuations (Les Houches Session LXIII)*, edited by S. Reynaud, E. Giacobino, and J. ZinnJustin (Elsevier, New York, 1997), pp. 351–386.
- [77] Y. Suzuki and K. Varga, *Stochastic Variational Approach to Quantum-Mechanical Few-Body Problems* (Springer, New York, 1998).
- [78] F. Neumann, G. Ingold, and H. Grabert, Influence of the environment on charge quantization in small superconducting islands, *Phys. Rev. B* **50**, 12811 (1994).
- [79] M. Carroll, S. Rosenblatt, P. Jurcevic, I. Lauer, and A. Kandala, Dynamics of superconducting qubit relaxation times, *npj Quantum Inf.* **8**, 132 (2022).
- [80] A. Blais, A. L. Grimsmo, S. M. Girvin, and A. Wallraff, Circuit quantum electrodynamics, *Rev. Mod. Phys.* **93**, 025005 (2021).
- [81] A. Harrow, Coherent communication of classical messages, *Phys. Rev. Lett.* **92**, 097902 (2004).
- [82] M. M. Wilde, H. Krovi, and T. A. Brun, Coherent communication with continuous quantum variables, *Phys. Rev. A* **75**, 060303(R) (2007).
- [83] E. Chitambar and M.-H. Hsieh, Relating the resource theories of entanglement and quantum coherence, *Phys. Rev. Lett.* **117**, 020402 (2016).
- [84] G. Vidal and R. F. Werner, Computable measure of entanglement, *Phys. Rev. A* **65**, 032314 (2002).

- [85] M. B. Plenio, Logarithmic negativity: A full entanglement monotone that is not convex, *Phys. Rev. Lett.* **95**, 090503 (2005).
- [86] K. Życzkowski, P. Horodecki, A. Sanpera, and M. Lewenstein, Volume of the set of separable states, *Phys. Rev. A* **58**, 883 (1998).
- [87] K. Życzkowski, Volume of the set of separable states. II, *Phys. Rev. A* **60**, 3496 (1999).
- [88] H. P. Breuer and F. Petruccione, *The Theory of Open Quantum Systems* (Oxford University Press, New York, 2002).
- [89] R. Alicki and K. Lendi, *Quantum Dynamical Semigroups and Applications* (Springer-Verlag, Berlin, 2007).
- [90] A. Rivas and S. F. Huelga, *Open Quantum Systems: An Introduction*, Springer Briefs in Physics (Springer, New York, 2012).
- [91] D. A. Lidar, Lecture notes on the theory of open quantum systems, [arXiv:1902.00967](https://arxiv.org/abs/1902.00967).
- [92] R. Jozsa, Fidelity for mixed quantum states, *J. Mod. Opt.* **41**, 2315 (1994).
- [93] J. L. Dodd and M. A. Nielsen, Simple operational interpretation of the fidelity of mixed states, *Phys. Rev. A* **66**, 044301 (2002).
- [94] Z.-H. Ma, F.-L. Zhang and J.-L. Chen, Metrics Of Quantum States, [arXiv:0812.3016](https://arxiv.org/abs/0812.3016).
- [95] A. Rivas, S. F. Huelga, and M. B. Plenio, Entanglement and non-markovianity of quantum evolutions, *Phys. Rev. Lett.* **105**, 050403 (2010).